Defect structure in transition-metal monoxides

P. K. Khowash and D. E. Ellis
Department of Physics and Astronomy, Northwestern University, Evanston, Illinois 60208
(Received 11 April 1988; revised manuscript received 26 September 1988)

The electronic structure and stabilization energy of metal vacancy and vacancy-interstitial clusters are studied in transition-metal monoxides using the first-principles local-density theory. The discrete-variational method in the embedded-cluster scheme is used to obtain both the one-electron properties and cohesive energies. Our calculations predict greater stability for 2:1 (vacancy:interstitial) defect structure over simple vacancies. This is in agreement with experiments for MnO and the heavier 3*d* compounds, but for TiO and VO lattice vacancies at the metallic or oxygen sites are experimentally predominant. The energy for the single metal vacancy is calculated to be close to the 2:1 defect energy, and so cluster-size effects and computational limitations need to be considered further. For FeO and CoO, however, the 4:1 interstitial complex is found to be more stable than other simple defects, in accord with experiment. The probability of formation of 4:1 clusters and their aggregates in TiO and MnO is explored; the interstitial metal ion tends to be in a trivalent state as previously determined for FeO and CoO.

I. INTRODUCTION

The transition-metal monoxides exhibit a rocksalt structure, with chemical valence corresponding to metal ions in a 2+ oxidation state in the ideal composition. Experiments like x-ray diffraction, neutron diffraction, diffuse x-ray scattering, electron microscopy, etc. performed over the past two decades on these oxides indicate a copious number of vacancies and interstitials, accompanying deviations from the stoichiometric structure. In spite of such extensive studies, the most stable defect structures are not well resolved due both to the difficulty in preparing well-characterized samples and ambiguities in fitting defect models to data. We make an energy analysis of the defect structures of transition-metal monoxides TiO and MnO here and make a direct comparison with the existing results for FeO (Ref. 1) and CoO (Ref. 2) to get a better insight of the nature of relative stability of various defects.

The local-density theory has been successfully used to study electronic properties of solids and their energetics using both band structure and cluster representations. The well-known band-structure methods can provide accurate total energies and density of states when the system has a periodic translational symmetry. The classic band theoretical calculations by Mattheiss[3] for the transition-metal oxides identify CaO to be an insulator and TiO, VO, MnO, FeO, CoO, and NiO to be metals. However, experimentally, MnO, FeO, CoO, and NiO are found to be antiferromagnetic insulators, leading to extensive discussions about the validity (or nonvalidity) of single particle methods in general, and band structure in particular, for description of strongly correlated electronic systems. Spin-polarized band-structure calculations[4,5] lead to a semiconductorlike behavior for MnO and NiO recovering some essential features.

The systems of our interest have vacancies at lattice sites and atoms in interstitial states. This breaks the periodicity of the solid, with effects which extend to several interatomic distances. Molecular cluster methods offer a convenient tool to study such localized properties for systems with low symmetry. Interactions with the bulk can be included by generating effective potentials due to host atoms around the chosen cluster, thereby minimizing surface and cluster-size effects.

II. THEORETICAL APPROACH

The discrete variational $X\alpha$ embedded-cluster method,[6–9] based on the local-density formalism, is used to calculate the ground-state electronic structure of ideal and defected clusters. For description of vacancies, "ghost" atoms with no nuclear charge but potential-well basis functions are introduced at the missing atom positions. The variational basis functions assigned are [Ar]3*d*4*s*4*p* for the metal atoms and [He]2*s*2*p*3*s*3*p* for oxygen and are generated by a self-consistent atom or ion in potential-well calculations. The wave functions, eigenvalues, and hence the Mulliken atomic orbital populations are then obtained by solving the Schrödinger equation self-consistently while enforcing the Pauli exclusion principle. The cluster embedding potential is generated by summing the charge density from 200–300 nearby host atoms in forming Coulomb and exchange-correlation potentials. Long-range electrostatic terms are included by Ewald summation.

The standard spin-polarized expression for the total energy in the local-density approximation is[10]

$$E_t=\sum_{\sigma}\left\{\sum_i f_{i\sigma}\varepsilon_{i\sigma}-\frac{1}{2}\int\int\frac{\rho_\sigma(\mathbf{r})\rho(\mathbf{r}')}{|\mathbf{r}-\mathbf{r}'|}d\mathbf{r}\,d\mathbf{r}'+\int\rho_\sigma(\mathbf{r})[E_{\mathrm{xc},\sigma}(\mathbf{r})-V_{\mathrm{xc},\sigma}(\mathbf{r})]d\mathbf{r}\right\}+\tfrac{1}{2}\sum_\mu\sum_\nu{}'\frac{Z_\mu Z_\nu}{r_{\mu\nu}}\,, \tag{1}$$

where the exchange-correlation energy $E_{xc,\sigma}(\mathbf{r})$ and the exchange-correlation contribution to the electronic potential $V_{xc,\sigma}(\mathbf{r})$ are related by

$$E_{xc,\sigma}(\mathbf{r})=\tfrac{3}{4}V_{xc,\sigma}(\mathbf{r}) \quad (2)$$

for the simplest Kohn-Sham potential. Total energies for even small clusters calculated in this manner are typically of the order of 10^5 eV, and are not determined accurately enough for direct comparison in the chosen numerical sampling scheme. It is possible, however, to extract sufficiently accurate binding energies by taking differences with respect to a reference system calculated on the same integration mesh,

$$E_B=E_t^{\text{sys}}-E_t^{\text{ref}} . \quad (3)$$

Since the spin-dependent exchange interaction contributes appreciably to isolated atom energies, the reference state of the separated atoms can best be treated by the spin-unrestricted density-functional formalism. Both $E_t[\rho]$ and $E_B[\rho]$ are found to be stationary with respect to the density ρ and the variational basis $\{\phi_i\}$.[19] The numerical error is minimized by computing the reference system energy over the same volume with the same sampling grid by freezing the atoms at their respective lattice sites but are now assumed to be noninteracting. This enables us to calculate cohesive energies with a precision of 0.01 eV, which is better than systematic sources of error such as basis truncation.

The statistical total-energy functional $E_t[\rho]$, with Kohn-Sham local exchange potentials, produces binding about 1% larger than the Hartree-Fock results in atoms and also exhibits overbinding in many molecules and solids. Errors in the calculation of total energy may arise not only from the inaccurate treatment of the exchange energy but also in numerical treatment of the deep-lying core levels. Since we are interested in comparison of systems whose core states are barely altered by interaction with the environment, this aspect of the problem is unimportant for a discussion of cohesion. Valence electron derived properties can be calculated consistently with reasonable effort, with an accuracy which greatly exceeds the absolute accuracy of either the atomic or the solid-state calculations.

III. RESULTS AND DISCUSSION

A. Background

The transition-metal monoxides showing metal deficiency over a large composition range are $Mn_{1-x}O$ $(0.001<x<0.15)$, $Fe_{1-x}O$ $(0.05<x<0.15)$, and $Co_{1-x}O$ $(0.001<x<0.05)$. On the other hand, TiO and VO (MO_x, $0.75<x<1.30$), at higher temperatures, exhibit vacancies on both metallic and oxygen sites even in the neighborhood of stoichiometry. In contrast to the pure NaCl structure stable above 1225 K, the crystal structure of TiO becomes more complex and of lower symmetry when annealed at lower temperatures. It is also highly brittle. Banus and Reed[11] calculate from their x-ray and pycnometric density measurements on TiO, that the defect concentration on the metallic and oxygen sites is nearly equal (15% each) assuming a random distribution among lattice sites.

X-ray diffraction studies on FeO (Ref. 12) indicate metal vacancies at the lattice site and introduction of metal ions at the tetrahedral interstitial position. The ratio (R) of the metal vacancy (m) to the interstitial (n) is critical for the defect structure and initially was proposed to be 2. Koch and Cohen[13] later confirmed the coexistence of vacancies and interstitials but proposed a different ($R=n:m$) ratio of 3. The observed superlattice reflections and Bragg peaks proved the defect clusters to be ordered. Experiments were performed at different partial oxygen pressures and it was later shown[14] that R decreases from 4 for $x=0.03$ to 3 for $x\cong 0.1$.

The high-temperature electrical properties measured[15] at various oxygen partial pressures indicate MnO to be an oxygen excess compound with the dominant defects being manganese vacancies. The hole concentration increases rapidly with temperature and is equal to the concentration of electrons at very low oxygen pressure. Again, the diffusion, oxidation, and thermogravimetric data[16] could be explained by ideal point defect theory, supporting the manganese vacancy model. The general defect structure was thus thought to be a single metal vacancy as was assumed for CoO in the same temperature range. On the other hand, Kofstad[17] interpreted his diffusion data on MnO by suggesting a 4:1 defect structure as seen in Wustite ($Fe_{1-x}O$). The neutron diffraction, magnetic susceptibility, and Mössbauer experiments[18] on MnO-FeO solid solutions suggest that the ratio of octahedral vacancy to the tetrahedral interstitial concentration in the two oxides is similar and therefore similar defect structure is expected for MnO as observed in FeO.

The number and type of defect structures found in CoO as a function of temperature and oxygen pressure were analyzed using the point defect model (single metal vacancy) by Dieckmann[19] in a study of electrical conductivity and cation tracer diffusion. Other measurements of electrical conductivity and thermoelectric power[20] suggest vacancy aggregates. Theoretical calculations reported recently[2] identify the 4:1 cluster to be most stable with the single vacancy lying proximately.

We report here the calculated metal vacancy and vacancy-interstitial defect structure of TiO and MnO and make an extensive comparison with the previously studied defect complexes in FeO and CoO.

B. Stoichiometric compound

To begin, we choose an eight atom cluster M_4O_4 by placing cations and anions at the corners of a cubic cell in tetrahedral symmetry for the stoichiometric solid. Each cluster atom is coordinated to three neighboring cluster atoms and three neighboring atoms in the crystal. The self-consistent charges and spins are shown in Table I. The calculated ionicities of the metal and oxygen ions are identical due to the stoichiometric nature of the cluster chosen. The self-consistent configurations of Ti $(3d^{1.66}4s^{0.12}4p^{0.34}4d^{0.06})$ and O $(2s^{1.77}2p^{4.68}3s^{0.04}3p^{0.90})$

TABLE I. Charge distribution (Mulliken net charges) and spin moment (μ_B) for ideal and different defect clusters as described in the text. V denotes a vacancy. The spin moment is given in parentheses.

	TiO	MnO	FeO	CoO
		Ideal structure (M_4O_4)		
M	1.81 (0.51)	1.47 (4.96)	1.89 (4.84)	1.38 (2.94)
O	−1.81 (0.04)	−1.47 (0.05)	−1.89 (0.12)	−1.38 (0.56)
		Metal vacancy 1:0 ($VO_6M_{12}O_8$)		
V	−0.82 (0.04)	−0.42 (0.00)	−0.39 (0.04)	−0.02 (0.01)
O(1)	−0.81 (−0.17)	−0.63 (0.05)	−1.63 (0.21)	−0.68 (0.44)
M	1.59 (1.53)	1.19 (0.23)	1.77 (4.29)	1.13 (2.83)
O(2)	−1.84 (0.49)	−1.66 (0.05)	−1.86 (0.03)	−1.74 (0.22)
		2:1 defect ($M_2V_2O_4M$)		
$M(1)$	1.21 (0.29)	1.24 (3.56)	1.84 (4.01)	0.98 (2.77)
V	−0.13 (0.00)	−0.09 (0.00)	−0.13 (0.01)	−0.11 (0.02)
O(1)	−1.87 (0.23)	−1.50 (0.47)	−1.72 (0.09)	−1.33 (0.47)
O(2)	−1.58 (0.03)	−1.22 (0.26)	−1.61 (0.13)	−1.08 (0.56)
$M(2)$	2.75 (1.43)	1.42 (2.27)	2.29 (3.87)	1.61 (3.14)
		4:1 defect (MO_4V_4)		
M	2.99 (0.09)	1.75 (4.27)	2.17 (4.30)	1.73 (2.90)
V	−0.24 (−0.03)	−0.05 (−0.03)	−0.12 (0.00)	−0.13 (−0.01)
O	−1.85 (0.45)	−1.27 (0.43)	−1.85 (0.02)	−1.17 (0.68)

are very similar to the band theoretical predictions[21] [Ti ($3d^{1.85}4s^{0.10}4p^{0.24}$); O ($2s^{1.71}2p^{4.19}3d^{0.25}$)]. The net magnetic moment calculated at the Ti site arising from the Ti $3d$ electrons in TiO is $0.51\mu_B$, which is consistent with the known weakly paramagnetic character of TiO. The calculated net spin $4.96\mu_B$ on Mn in MnO is in excellent agreement with the band theoretical result[5] of $5.0\mu_B$ and experimental[22] value of $4.79\mu_B$. To extract the antiferromagnetic structure in these series of materials, a cluster large enough to include the magnetic unit cell needs to be considered. It has been shown earlier[23] in FeO that the superlattice is essential for an accurate spin distribution while most of the other features are well represented by considering a single unit cell.

Figure 1 shows the calculated variation of binding energy as a function of the lattice parameter for TiO, MnO, FeO, and CoO. The binding energies at the experimental lattice constants are −14.2, −20.0, −18.1, and −13.3 eV and agree fairly well with the experimental values[24] of −13.4, −15.6, −22.6, and −17.5 eV, respectively. For FeO, however, the binding energy reported by Press and Ellis[1] is in error by a factor of 2 due to the fact that a minimal basis set was used in their calculations. Use of an extended basis function for FeO enhances the binding energy to −18.1 eV. This shows the sensitiveness of the binding energy to the basis functions used: a minimal basis yields ~50% of the experimental estimates, while an extended basis yields ~80% of the experimental value. The present results could be improved further by optimizing the basis sets. The experimental lattice parameters lie within 2–3 % of our embedded-cluster model predictions. The theoretical binding energies at the theoretical equilibrium position are −14.3, −20.4, −18.5, −14.5 eV for TiO, MnO, FeO, and CoO, respectively. The binding energy versus lattice parameter diagram was fitted to a parabola in order to calculate the bulk modulus defined as

$$B = V(\partial P/\partial V)_T$$

in these materials. The calculated values corresponding to TiO, MnO, FeO, and CoO are 0.6, 0.2, 0.9, and 1.4 Mbar. Unfortunately, no experimental data seem to exist to compare with our calculated results. To get a feeling

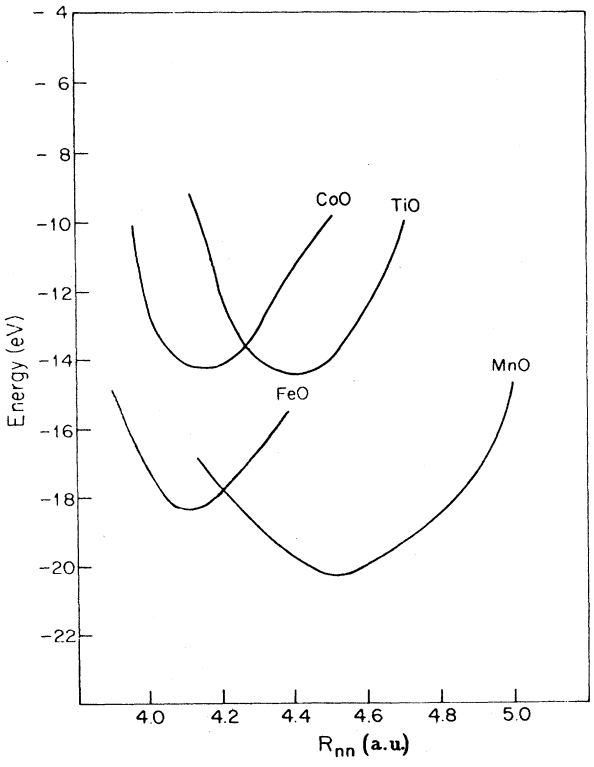

FIG. 1. Binding energy vs lattice parameter for TiO, MnO, FeO, and CoO.

for the magnitude, we consider the experimental bulk modulus values of some known materials. The bulk moduli of CuCl and CuBr are 0.38 and 0.39 Mbar,[25] while the bulk moduli of FeS_2, CoS_2, and NiS_2 are reported[26] to be 1.18, 1.15, and 0.94 Mbar, respectively. Thus the monoxides are here predicted to be intermediate between the easily deformed cuprous halides and ratherhard transition-metal disulphides. By further comparison, the modulus of bcc iron is 1.68 Mbar.[27]

C. Isolated metal vacancy

A vacancy is now created at a metal site: V identifies the vacancy in Table I. This vacancy is well coordinated by 6 oxygen atoms [O(1)], twelve metallic atoms (M) in the second shell, and 8 distant oxygen atoms [O(2)] in an octahedral configuration, for a total 27 atoms in the cluster. The vacancy in TiO picks up a larger charge as compared to the vacancies in other transition-metal oxides studied. O(1) in FeO picks up more charge as compared to others. This O(1) charge-up is probably due to the usage of a minimal basis set for FeO (Ref. 1) and thereby not allowing much charge to diffuse away from its ionic configuration. The overall ionicity on oxygen is close to the metal ionicity in all the cases, since the cluster charge was chosen on the basis of nominal valency. However, the oxy-anions close to the vacancy are significantly perturbed.

D. (2:1) defects

In the 2:1 defect structure, ($M_2V_2O_4M$), O(1), and O(2) identify oxygens close to a cation and vacancy, respectively, in Table I. $M(1)$ is the transition-metal atom at a regular lattice site and $M(2)$ identifies the interstitial atom at the tetrahedral site. The ionicity of the oxygen close to the vacancy is less than the ionicity of the oxygen close to a cation. This trend is also obvious from our single vacancy results. The ratio of the ionicities of $M(2)$ to $M(1)$ is 2.3, 1.1, 0.8, and 1.6 for Ti, Mn, Fe, and Co, respectively, thus spanning the value of 1.5, expected for 3+/2+ formal valency. Because of the almost half-filled 3d shell, the magnetic moment of the metal at a regular lattice site is slightly larger for MnO and FeO. The oxygens close to the vacancy, however, have lower moments in the cases of TiO and MnO only.

E. (4:1) defects

Finally, in the 4:1 defect complex the vacancy as usual picks up a little charge ranging from 0.05e to 0.24e. The net charge on the oxygen sites differ from their ideal ionicity by few tenths of an electron in all cases. The charge donated by the transition-metal atom at the interstitial tetrahedral site monotonically increases as we go from 1:0 (single metal vacancy) to the 4:1 defect via 2:1 defect structure by systematic removal of the metal ions, indicating the formation of the trivalent state, or in case of Ti, the tetravalent state, as observed experimentally. As is usual in Mulliken atomic orbital analysis, the full ionic charge is not attained.

F. Relative stability of defect structures

It has been stated earlier that the transition metal monoxides form with single vacancies (Ti,V,. . .) and/or vacancy-interstitial aggregates (. . . ,Mn,Fe,Co). Most of the later experiments suggest the defect clustering to be of 4:1 nature. Extensive theoretical and experimental studies exist for these monoxides in the literature.[1–4,12–14,21,28–35] In comparing various defect energies, we start with a single vacancy and then consider successively more complex vacancies created by systematic removal of metal ions and translation to interstitial sites. In the process of removal of metal atoms one after the other to create vacancies, the cluster becomes charged. The charge neutrality is, however, maintained by proper positioning of Fe^{3+} ions in the microcrystal generated around the cluster. Since a direct comparison of the absolute binding energies of the different defect complexes of different sizes does not make much sense, we report the binding energy per net number of vacancies and plot our data in a relative scale with respect to the ideal structure. The complex defects considered generally can be thought of as formed from vertex-, edge-, or face-shared composites of the basic 4:1 interstitial cluster. The 3:2 complex discussed below as calculated in C_{3v} symmetry corresponding to the open structure vertex-shared (2:1) pair with vacancies only on the (111) symmetry axis.

In TiO, the 2:1 defect structure is found to be most stable with the single vacancy energy lying close by ($\Delta E = 0.54$ eV), as shown in Fig. 2. In contrast, the band-structure calculation of Huisman *et al.* yields no net stabilization due to single vacancies.[21] The 3:2 defect also shows a slight excess binding against other complex defects. The 6:2 defect shows a local minimum as we go on removing metal atoms but is not energetically favorable as compared to the ideal structure to form a stable defect structure. MnO shows somewhat similar trends: The relative binding energy falls rapidly as the number of metal vacancies increases. A drop in energy is seen at 6:2, giving rise to a locally stable minimum. The single vacancy and the 2:1 energies are very close ($\Delta E = 0.15$ eV) and suggest that both defect structures can coexist with the probability of 2:1 being slightly larger. The defects chosen by Keller and Dieckmann[28] were ideal neu-

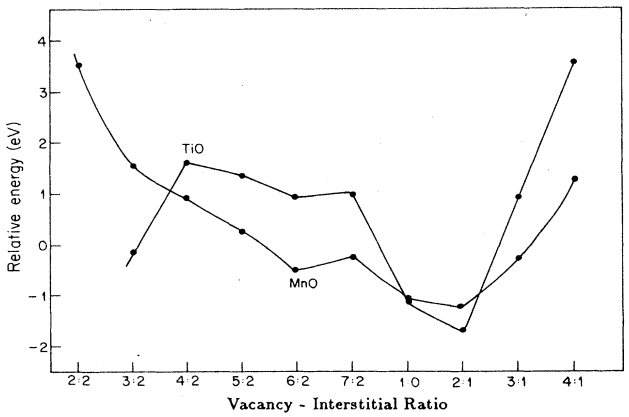

FIG. 2. Relative energy of various defects in TiO and MnO. The straight lines between the calculated $m:n$ points are a guide to the eye.

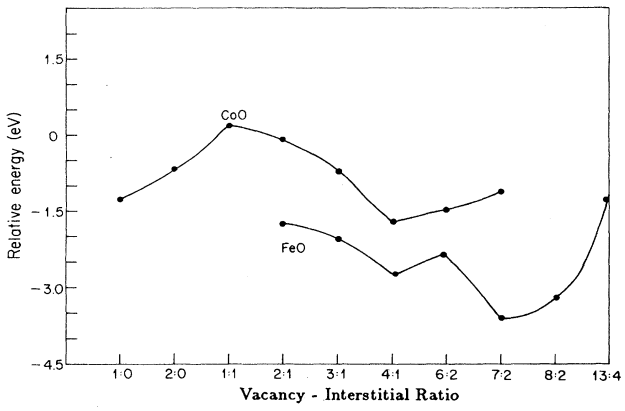

FIG. 3. Relative energy of various defects in FeO and CoO. The straight lines between the calculated $m:n$ points are a guide to the eye.

tral, and singly, and doubly charged vacancies. This model fits the nonstoichiometry data well but not the electrical data. Recent thermoelectric power and electrical conductivity measurements on MnO were used to identify a plausible defect model.[36] By fitting the experimental data to the different defect models, a cluster interpreted to be of $m-n=1$ (vacancy minus interstitial) (i.e., 2:1, 3:2, etc.) nature[36] emerged. This data led to an activation energy[37] which also showed that a neutral cluster of $m-n=1$ was energetically favored over a charged cluster, with mobile holes as charge compensators. This is in agreement with our calculated 2:1 defect structure. The mobile holes can be related to the trivalent metal atoms introduced in the microcrystal as charge compensators in our calculations.

We take the data for FeO (Ref. 1) and CoO (Ref. 2) obtained from the embedded-cluster calculations performed earlier and plot them in a relative energy scale in Fig. 3. It was seen that in $Fe_{1-x}O$, a "ferric" species in the tetrahedral site stabilizes the defect structure to a larger extent as compared to any combination of vacancies and octahedral Fe^{3+} ions. The 4:1 defect is stable with respect to smaller defect complexes, but more stable configurations are possible by edge sharing of these 4:1 defects to generate 7:2 defects. In $Co_{1-x}O$, however, we find that the system prefers to form a single isolated vacancy first and then evolve to a 4:1 defect structure. This also indicates why the single metal vacancy model could account for much of the experimental data in the past. The general consensus is that the light transition metals prefer to generate a single vacancy first and then settle at different defect structures like 2:1, 4:1, or their aggregates.

IV. CONCLUSION

The electronic structure and cohesive energy of single defects and defect clusters were studied in transition-metal oxides using the discrete variational linear combination of atomic orbitals approach in the embedded-cluster scheme. Our calculations predict greater stability for the 2:1 defect structure over other possible simple defects. This is in agreement with experiments for MnO but at either end of the $3d$ series the model fails. For TiO a lattice vacancy at the metallic site or oxygen site is experimentally predominant. The calculated theoretical energy for a single vacancy lies close to the 2:1 defect energy, so further calculations on larger clusters with refined bases need to be considered. It should also be noted that the lattice was frozen in our calculation of cohesive energies for the different defect clusters. Local lattice relaxation could lead to a reordering of relative energies. For FeO and CoO, we find that the 4:1 defect structure is more stable than simpler defects. The 4:1 defect clusters in TiO and MnO are found to be unfavorable, with respect to both 1:0 (single vacancy) and 2:1 defects.

The present data can be useful in selecting models to fit x-ray diffuse scattering, thermopower, electrical conductivity, and related transport data. In principle they can be incorporated in thermodynamic models such as the cluster variational method of Kikuchi[38] to predict thermal variation of defect concentrations and contributions to transport and diffusion coefficients.

ACKNOWLEDGMENT

This work was supported by the U.S. Department of Energy, under Grant No. DE-FG02-86-56097-A01.

[1]M. R. Press and D. E. Ellis, Phys. Rev. B **35**, 4438 (1987).
[2]P. K. Khowash and D. E. Ellis, Phys. Rev. B **36**, 3394 (1987).
[3]L. F. Mattheiss, Phys. Rev. B **5**, 306 (1972).
[4]T. M. Wilson, J. Appl. Phys. **40**, 1588 (1969); Int. J. Quant. Chem. **53**, 757 (1970).
[5]T. Oguchi, K. Terakura, and A. R. Williams, Phys. Rev. B **28**, 6443 (1983).
[6]E. J. Baerends, D. E. Ellis, and P. Ros, Chem. Phys. **2**, 41 (1973).
[7]A. Rosén, D. E. Ellis, H. Adachi, and F. W. Averill, J. Chem. Phys. **65**, 3629 (1982).
[8]D. E. Ellis and G. L. Goodman, Int. J. Quant. Chem. **25**, 1949 (1982).
[9]B. Delley and D. E. Ellis, J. Chem. Phys. **76**, 1949 (1982).
[10]B. Delley, D. E. Ellis, A. J. Freeman, E. J. Baerends, and D. Post, Phys. Rev. B **27**, 2132 (1983).
[11]M. D. Banus and T. B. Reed, in *The Chemistry of Extended Defects in the Non-Metallic Solids,* edited by L. Eyring and M. O'Keeffe (North-Holland, Amsterdam, 1970), p. 488.
[12]W. L. Roth, Acta Crystallogr. **13**, 140 (1960).
[13]F. Koch and J. B. Cohen, Acta Crystallogr. Sect. B **25**, 275 (1969).
[14]A. K. Cheetham, B. E. F. Fender, and R. I. Taylor, J. Phys. C **4**, 2160 (1971).
[15]A. Z. Hed and D. S. Tannhauser, J. Chem. Phys. **47**, 2090 (1967).
[16]J. Bransky and N. M. Tallan, J. Electrochem. Soc. **118**, 788 (1971).
[17]P. Kofstad, J. Phys. Chem. Solids **44**, 879 (1983).
[18]D. A. O. Hope, A. K. Cheetham, and G. J. Long, Inorg.

Chem. **21**, 2804 (1982).
[19]R. Dieckmann, Z. Phys. Chem. **107**, 189 (1978).
[20]E. M. Logothetis and J. K. Park, Solid State Commun. **43**, 543 (1982).
[21]A. Neckel, P. Rastl, R. Eibler, P. Weinberger, and K. Schwarz, J. Phys. C **9**, 579 (1976); L. M. Huisman, A. E. Carlsson, C. D. Gelatt, Jr., and H. Ehrenreich, Phys. Rev. B **22**, 991 (1980).
[22]B. E. F. Fender, A. J. Jacobson, and F. A. Wedgewood, J. Chem. Phys. **48**, 990 (1968).
[23]S. H. Chou, J. Guo, and D. E. Ellis, Phys. Rev. B **34**, 12 (1986).
[24]T. C. Waddington, Adv. Inorg. Chem. Radiochem. **1**, 157 (1959).
[25]M. R. Press and D. E. Ellis, Phys. Rev. B **38**, 3102 (1988).
[26]G. Will, J. Lauterjung, H. Schmitz, and E. Hinze, Mater. Res. Soc. Symp. Proc. **22**, 49 (1984).
[27]A. V. Gold, L. Hedge, P. T. Pánonsis, and D. R. Stone, Int. J. Magn. **2**, 357 (1971).
[28]M. Keller and R. Dieckmann, Ber. Bunsenges Phys. Chem. **89**, 1095 (1985).
[29]C. R. A. Catlow, W. C. Mackrodt, M. J. Norgett, and A. M. Stoneham, Philos. Mag. **40**, 161 (1979).
[30]R. Tetot and P. Gerdanian, J. Phys. Chem. Solids **46**, 869 (1985).
[31]D. E. Eastman and J. L. Freeouf, Phys. Rev. Lett. **34**, 395 (1975).
[32]K. Terakura, T. Oguchi, A. R. Williams, and J. Kübler, Phys. Rev. B **30**, 4734 (1986).
[33]F. W. Kutzler and D. E. Ellis, Phys. Rev. B **29**, 6890 (1984).
[34]C. R. A. Catlow and A. M. Stoneham, J. Amer. Ceram. Soc. **64**, 4 (1981).
[35]M. D. Banus, T. B. Reed, and A. J. Strauss, Phys. Rev. B **5**, 2775 (1972).
[36]G. P. Sykora, Ph.D. thesis, Northwestern University, 1987.
[37]G. P. Sykora and T. O. Mason, Mater. Res. Soc. Symp. Proc. **60**, 243 (1986).
[38]R. Kikuchi, Phys. Rev. **81**, 988 (1951).